Rhamnazin Enhanced Anti-Tumor Efficacy of Anti-PD-1 Therapy for Lung Cancer in Mice through Inhibition of PD-L1 Expression

Shu Shi Wang,[1] **Ye Liu,**[2] **Xuan Ting Zhang**[3] **and Dong Qiang Yu**[4]

[1]Department of Oncology, Zouping People's Hospital, Zouping, Shandong, China
[2]Health Institute of Shandong Labor Vocational and Technical College, Jinan, Shandong, China
[3]Department of Respiratory and Critical Care Medicine, Qingdao Central Hospital Affiliated to Qingdao University, Qingdao, Shandong, China
[4]Department of Emergency Internal Medicine, Affiliated Hospital of Qingdao University, Qingdao, Shandong, China

Emerging studies suggest the significance of broadening the benefit of anti-programmed cell death 1 (PD-1) therapy for lung cancer. The anti-angiogenic agents have been reported to alter the tumor microenvironment and contributes to efficiency of anti-PD-1 therapy. This study aims to investigate whether the anti-angiogenic agent rhamnazin enhances the efficacy of anti-PD-1 therapy in lung cancer. In Lewis lung carcinoma (LLC) xenografts, the combination of rhamnazin and anti-PD-1 treatment suppressed tumor growth, elevated the infiltration of CD4$^+$ T and CD8$^+$ T cells in tumors and up-regulated interferon-gamma (IFN-γ), tumor necrosis factor alpha (TNF-α), and granzyme B. Furthermore, the combination reduced programmed cell death ligand 1 (PD-L1) expression in tumors more significant than anti-PD-1 treated group. In LLC cell experiments, rhamnazin inhibited vascular endothelial growth factor A (VEGFA)-stimulated vascular endothelial growth factor receptor 2 (VEGFR2) phosphorylation and PD-L1 expression, whereas VEGFR2 overexpression reversed these trends. T cell proliferation and cytotoxic factor production were evaluated after co-culturing with non-small cell lung cancer (NSCLC) H1975 cells. Rhamnazin promotes T cell proliferation and up-regulated IFN-γ, TNF-α and granzyme B in the co-culture system, while VEGFR2 overexpression abrogated these changes. These data suggest that rhamnazin enhances anti-tumor effect of anti-PD-1 therapy for lung cancer in mice via inhibition of PD-L1 expression.

Introduction

Lung cancer is emerging as a leading cause of cancer-related deaths worldwide, among which non-small cell lung cancer (NSCLC) accounts for approximately 85% of total lung tumors (Relli et al. 2019; Yu and Li 2020). In clinical, the target oncogene therapy such as epidermal growth factor receptor (EGFR) mutations, blocking the interaction between PD-1 and its ligand PD-L1, and anti-angiogenic monoclonal antibodies (mAb) treatment are popular for advanced NSCLC (Losanno et al. 2016; Xia et al. 2019). The clinical trials have confirmed that the PD-1/PD-L1 blocking therapies lead to higher overall survival in patients with advanced NSCLC (Vansteenkiste et al. 2019). Recently, the new therapeutic methods of combined immunotherapies and conventional treatments were reported to extend the benefits of patients with lung cancer.

Previous reports have shown that PD-1/PD-L1 mAbs have poor efficacy in non-inflammatory tumors, which are characterized by poor lymphocyte infiltration, increased immunosuppressive components, and abnormal angiogenesis in the tumor microenvironment (TME) (Hegde et al. 2016; Chen and Mellman 2017). The combining anti-PD-1 mAbs and agents can modulate the immunosuppressive environment of TME and may overcome treatment resistance of advanced NSCLC patients (Mahoney et al. 2015). Anti-angiogenic therapy for TME of NSCLC is mainly targeting the pro-angiogenic factor vascular endothelial growth factor (VEGF) and its receptor 2 (VEGFR2) (Volz et al. 2020). VEGFR2 plays a crucial role in mediating the

mitogenesis and permeability of endothelial cells (Belgore et al. 2004), and the activation of VEGFR2 contributes to phosphorylation of multiple downstream signaling molecules that subsequently promote tumor growth (Chen et al. 2020a). VEGFR2 has become an important therapeutic target for cancer anti-angiogenesis therapy, and some small molecular inhibitors of VEGFR2 have been employed in clinical trials, such as sunitinib, vandetanib, and sorafenib (Chang et al. 2013; Hu et al. 2019). A total of 11 anti-angiogenic agents, including anti-VEGF antibody, anti-VEGFR antibody, as well as VEGFR tyrosine kinase inhibitors (TKIs), have been approved for certain types of cancer. However, continued clinical and preclinical investigations have identified major drawbacks associated with the application of this class of agents, including inherent/acquired resistance and high frequency of bleeding complications (Elice and Rodeghiero 2012).

Chinese medicine is an important component of comprehensive treatment measures for malignant tumors due to its low intrinsic toxicity. Rhamnazin, a polyphenolic compound, is often extracted from medicinal plants such as ginkgo biloba, willow and sea buckthorn (Yu et al. 2018). Previous evidence has indicated that rhamnazin contributes to immune regulation and anti-tumor effects (Martini et al. 2004). Rhamnazin is also a VEGFR2 signaling inhibitor which involves in inhibiting the phosphorylation of VEGFR2 and its downstream signaling regulators, thereby processing anti-tumor effects in breast cancer (Yu et al. 2015). In view of the recent studies demonstrated that the combination of immunotherapies and conventional treatments enlarge the benefits to patients with cancers (Yasuda et al. 2013; Cai et al. 2020), it is of considerable significance to study whether the rhamnazin combined with anti-PD-1 therapy can indeed improve the treatment efficacy of lung cancer.

In this study, we established Lewis lung carcinoma model in C57BL/6 mice and analyzed the treatment efficacy of combined rhamnazin and anti-PD-1 therapy. We also assessed the impact of rhamnazin on PD-L1 expression in NSCLC cells and the regulatory mechanism. Our research may provide valuable evidence for the exploration of combination of immunotherapies and conventional treatments in lung cancer.

Material and Methods

Cell line, culture and rhamnazin preparation

Lewis lung carcinoma (LLC) cell line and NSCLC cell line H1975 were purchased from American Type Culture Collection (ATCC, Rockville, MD, USA) and cultured in RPMI-1640 medium (Gibco, Grand Island, NY, USA) containing 10% fetal bovine serum (FBS, Gibco), 100 U/mL of penicillin, and 100 μg/mL of streptomycin (Gibco) in the presence of 5% CO_2 at 37°C. Rhamnazin (98%, Sigma, St. Louis, MO, USA) was dissolved in dimethyl sulfoxide (DMSO) to prepare required concentrations.

Cell transfection

Short hairpin RNA (shRNA) of VEGFR2 (sh-VEGFR2) was obtained from GenePharma Co., Ltd. (Shanghai, China). Non-target shRNA control (sh-NC) was used as negative control. For the overexpression of VEGFR2, full-length human VEGFR2 (VEGFR2-OE) was cloned into a pEX-3 vector (GenePharma). The empty vector was used as the control. Cellular transfection was performed by using Lipofectamine 3000 (Invitrogen, Carlsbad, CA, USA) for 48 h. Subsequently, these cells were collected for western blotting analysis.

Lewis lung cancer model

C57BL/6 mice (6-8 weeks old, male) were purchased from Shanghai Slake Laboratory Animal Co., Ltd (Shanghai, China). Mice were raised in specific pathogen-free environment and optimal conditions of light, temperature, and humidity and given free food and water. To induce a subcutaneous tumor model, a total of 1×10^6 LLC cell suspensions in 100 μL phosphate-buffered saline (PBS) were prepared and inoculated subcutaneously into the right flank of mice. When tumors reached approximately 100 mm^3, the daily intragastric administration of 200 mg/kg rhamnazin or carboxy methylated cellulose (vehicle) was carried out for consecutive 25 days (six mice in each group). After intragastric administration for 6, 13, and 20 days, mice were given 0.25 mg/kg anti-PD-1 monoclonal antibody (RMP1-14, BioXcell, West Lebanon, NH, USA) via intraperitoneal injection. The tumor volumes were measured every 3 days by caliper measurements and calculated based on the formula: tumor volume (mm^3) = [(length × width^2)/2]. The mice were sacrificed after intragastric administration on day 25, and the tumors were then removed for taking photos, volume measurement, quantitative real-time PCR or western blot assay. The tumor growth inhibition rate was calculated as follows: (1 − Wt/Wc) × 100%, where Wt is the tumor weight of each treatment group, and Wc is the tumor weight of the control group. The animal experimental procedures were conducted following the guidance of the National Institutes of Health and approved by the Animal Ethics Committee of Affiliated Hospital of Qingdao University.

Chicken chorioallantoic membrane (CAM) assay

Day-6 fertilized chicken eggs (Yueqin Breeding Co., Ltd, Guangdong, China) were chosen to perform the CAM assay. To expose the CAM, a window about 2 cm in diameter was opened in the eggshell. A sterile filter paper in 0.5 cm diameter was placed on the CAM before 20 μM rhamnazin or vehicle was added. The window was closed using a piece of steriled adhesive tape, and eggs were placed in a 37°C incubator with 80-90% relative humidity for 3 days. CAMs were fixed by stationary solution (methanol:acetone = 1:1) for 15 min and photos were taken by a digital camera.

Immunohistochemical (IHC) staining

The angiogenesis in tumors was analyzed by IHC staining with anti-platelet endothelial cell adhesion molecule (CD31). Briefly, the tumor tissues were fixed with formalin, embedded, cut into 5-μm sections, deparaffinized, and rehydrated in a graded series of ethanol. To block endogenous peroxidase, sections were immersed in with 3% hydrogen peroxide for 30 min at room temperature. The sections were then stained with primary antibodies containing mouse anti-CD31 (#ab182981, 1:2,000, Abcam, Cambridge, UK), anti-CD4 (#ab288724, 1:1,000, Abcam) and anti-CD8 (#ab237723, 1:500, Abcam). Sections were washed three times in PBS, each for 5 min duration, and then incubated with secondary antibody for 2 h at room temperature. The tumor vessel densities were calculated based on the number of CD31-positive luminal structures. Six random fields under a light microscope (Olympus CX31, Tokyo, Japan) of each section were captured. Three sections of each sample were collected for the qualification (Zhao et al. 2019).

Tumor-infiltrating lymphocytes (TILs)

After tumors were harvested from individual mice, 2 cubic millimeters of tumor were separated from the whole tumor and were frozen in liquid nitrogen for gene expression analysis. Single-cell suspensions were generated through enzymatic digestion at 37°C for 1 h in DMEM medium containing collagenase type IV (1 mg/mL, Sigma), hyaluronidase (1 mg/mL, Sigma) and DNase I (20 U/mL, Sigma) from the collected tissues. Erythrocytes were lysed in the Red Blood Cell Lysis Buffer (Sigma). The single cell samples were stained with antibodies containing anti-CD4, anti-CD69, anti-CD8 and anti-PD-L1 (Thermo Fisher, Waltham, MA, USA) in the dark for 30 min at 4°C. For the intracellular marker staining, cells were fixed and permeabilized with anti-Ki-67 antibody (MA5-14520, Invitrogen, Waltham, MA, USA) in the dark for 30 min at 4°C. Then, the stained single cell suspensions were washed twice with PBS, re-suspended in 500 μl PBS, and subjected to flow cytometry analysis. The percentage of positive staining cells, determined over 10,000 events, was analyzed using a FACS Calibur flow cytometer (Becton Dickinson, Franklin Lakes, NJ, USA).

Quantitative real-time PCR (qRT-PCR)

Total RNA was extracted from LLC cells or tumors using the Trizol Reagent (Invitrogen). The purity and quality of total RNA was identified by agarose gel electrophoresis and nucleic acid detection instrument. Equal amount (1 μg) of RNA was reverse-transcribed into cDNA with the MasterMix First Strand cDNA Synthesis Kit (Tiangen, Beijing, China). Relative expressions of CD4 and CD8 in tumor tissues and PD-L1 expression in H1975 cells was determined by performing the qRT-PCR in the Applied Biosystems 7500 system with the SYBR Premix ExTagTM (Takara, Shiga, Japan). The gene expression levels were normalized to GAPDH, and $2^{-\Delta\Delta CT}$ method was employed to calculate relative gene mRNA levels. The sequences of primers used are the following: CD4 forward primer: 5′-GCTGGAATCCAACATCAAGG-3′, CD4 reverse primer: 5′-CTTCTGAAACCGGTGAGGAC-3′; CD8 forward primer: 5′-AGCCACGTCAACAAGGACAT-3′, CD8 reverse primer: 5′-ACGATGGTGACGATCAGAGC-3′; GAPDH forward primer: 5′-ACAACTTTGGTATCGTGGAAGG-3′, GAPDH reverse primer: 5′-GCCATCACGCCACAGTTTC-3′.

Enzyme linked immunosorbent assay (ELISA)

After finishing the specific treatment, the supernatants of co-culture system were collected and centrifuged at 2,000 rpm for 5 min to remove the cell debris. Tumor tissues from mice were homogenized and extracted in lysis buffer (Beyotime) followed by centrifugation at 15,000 g for 20 min to isolate protein. The concentrations of IFN-γ, TNF-α and granzyme B in cell supernatants and tumor tissues were evaluated by the commercial ELISA kits purchased from Beyotime according to the standard protocols provided by the manufacturer. Briefly, the collected supernatants were incubated with reaction solution followed by the incubation in stop solution, the optical density (OD) value was measured under a microplate reader (Molecular Devices, Sunnyvale, CA, USA) at 490 nm to evaluate concentrations of relative factors.

Western blot

Proteins in H1975 cells and homogenized tumor tissues were extracted in lysis buffer (Beyotime). The concentration was measured by using BCA protein kit (Beyotime). Extracted proteins were separated by 10% SDS-polyacrylamide gel electrophoresis and transferred to PVDF membrane (Bio-Rad, Hercules, CA, USA). 1 h after blocking in Tris-buffered saline (TBS) buffer containing 5% nonfat milk, the membranes were incubated with primary antibodies anti-p-VEGFR2 (#3770, 1:1,000, Cell Signaling Technology, Danvers, MA, USA), anti-VEGFR2 (#ab2349, 1:1,000, Abcam) and anti-PD-L1 (#ab213480, 1:1,000, Abcam) at 4°C overnight. After washing 3 times using TBS buffer, the membranes were incubated with horseradish peroxidase (HRP)-conjugated goat anti-rabbit IgG secondary antibody (#A0208, 1:10,000, Beyotime) at room temperature for 2 h. The protein signals were visualized by the enhanced chemiluminescence (ECL) detection system (Amersham, Bucks, UK).

Cell counting Kit-8 (CCK8) assay

A CCK-8 kit (Dojindo, Shanghai, China) was used to measure T cell proliferation. Briefly, a total of 1×10^3 cells were seeded in 96-well plates in a volume of 100 μl per well. After finishing the treatment of anti-CD3 antibody (1 μg/mL) or rhamnazin (20 μM), cells were cultured for 1 day, 2 days, 3 days, 4 days and 5 days. Then, the CCK-8 reagent (10 μL) and 90 μL RPMI-1640 were added to each well and incubated for 2 h. The absorbance values at

490 nm were measured using an enzyme immunoassay analyzer (Thermo Fisher). The cell viability of H1975 or LLC was also evaluated using a CCK-8 kit and 50% inhibitive concentration (IC50) of rhamnazin was examined.

Isolation of human peripheral blood mononuclear cells (PBMCs)

PBMCs were purchased from TPCS (Milestone Biotechnologies, Shanghai, China). Total T cells were negatively selected from PBMCs by CD3 magnetic negative selection using EasySep Human T Cell Isolation Kit (Cat#17951, STEMCELL Technologies, Cologne, Germany). Human primary T cells were cultured in X-VIVO™15 medium (Cat#: BE02-060F, Lonza Group, Basel, Switzerland) with 5% FBS and 200 U/ml IL-2 (Cat#PHC0026, Thermo Fisher). To activate T cells, a total of 3 million $CD3^+$ T cells were treated by anti-CD3 magnetic Dynabeads (Thermo Fisher). After 48 h, activated T cells were maintained by culture medium previously described at a density of 1 million cells per ml of culture medium and change the fresh medium every 2-3 days. Institutional review board approval and patient informed consent were obtained.

T cell cytotoxicity in vitro

To validate the effect of primary T cells on cancer cells, we co-cultured primary T cell with cancer cells. H1975 cells (5×10^4) were seeded into 12 well-plates overnight, then the next day incubated with activated T cells by the ratio of H1975 cells to T cells 1:5 for 24 h at the treatment of rhamnazin. Next, T cells were collected, and its proliferation was determined using CCK-8 assay. The concentrations of IFN-γ, TNF-α and granzyme B in cell supernatants were evaluated by the commercial ELISA kits.

Statistical analysis

The data were presented as mean ± standard deviation (SD), and analyzed using SPSS 16.0 software (SPSS Inc., Chicago, IL, USA). Student's t test was used to analyze the significance between two groups. Comparisons among multiple groups were evaluated by one-way ANOVA test. The differences with $p < 0.05$ are considered statistically significant.

Results

Rhamnazin inhibits tumor growth and reduces angiogenesis in tumors with PD-1 blockade

Increasing studies have demonstrated the anti-tumor effect of rhamnazin or anti-PD-1 therapy in various cancers (Chen and Han 2015; Mei et al. 2022). We began our research by scheduling rhamnazin administration and investigated the changes in NSCLC H1975 or Lewis lung carcinoma (LLC) cell proliferation. Rhamnazin had the potential to inhibit the growth of H1975 and LLC cell with IC50 values of 17.7 μM and 23.5 μM, respectively (Fig. 1A, B). To assess the impact of rhamnazin combined with anti-

PD-1 therapy on lung cancer, we evaluated its influences on tumor growth and anti-angiogenic activity. LLC xenografts were established by subcutaneous inoculation of LLC cells followed by anti-PD-1 or rhamnazin administration. The schematic diagram of cell inoculation and treatment was displayed in Fig. 1C. As indicated in Fig. 1D, either anti-PD-1 or rhamnazin treatment showed significant inhibitory effects on tumor growth when compared to the vehicle group. Moreover, it was observed that the combination uses of rhamnazin and anti-PD-1 inhibited the tumor growth more significant than anti-PD-1 or rhamnazin treatment alone. Similarly, the tumor weight was decreased after treatment of anti-PD-1 or rhamnazin, and the combination group reduced more than individual groups (Fig. 1E). The tumor inhibition rate of each group was 42.3 ± 7.2% in the rhamnazin group, 57.5 ± 8.9% in the anti-PD-1 group, and 76.8 ± 4.9% in the combination group. These data suggest that rhamnazin elevates the antitumor efficacy of anti-PD-1 therapy in LLC model mice. Next, the angiogenesis in tumors was analyzed by immunohistochemical staining with anti-CD31 antibody. According to the detection results, anti-PD-1 therapy had no significant effect on angiogenesis, showing no noticeable change of CD31 protein level between anti-PD-1 and vehicle group. Different to this, the rhamnazin alone or combined treatment dramatically induced a substantial anti-angiogenic effect compared to vehicle or anti-PD-1 group, as evidenced by the decreased CD31 protein level in tumors (Fig. 1F, G). Consistent with CD31 staining assay, results in Fig. 1H further corroborated that rhamnazin strongly inhibited the angiogenesis in CAM assay. Anti-angiogenic therapy can cause a temporary reversion of tumor vessels towards a normalized structure and function. Hypoxia activates hypoxia-inducible factor-1α (HIF-1α) can adjust VEGFA and is essential for triggering vascular growth and improving oxygen supply in response to oxygen deficiency. When compared to tumor tissue from mice treated with vehicle, qRT-PCR results showed that there was no discernible change in the gene expression of HIF-1α in the rhamnazin group (Fig. 1I). Thus, rhamnazin enhanced the anti-tumor effect in tumor growth and angiogenesis in tumors with PD-1 blockade in LLC-xenografted mice.

Rhamnazin enhances T cell infiltration and activates local immune status in tumors with PD-1 blockade

Having found the improving benefit of rhamnazin on anti-PD-1 therapy, we next investigated how the combined therapy impacted T cell infiltration and local immune response. The $CD4^+$ T and $CD8^+$ T cell infiltration in tumor tissues was examined by IHC and qRT-PCR analysis. Based on the IHC staining data, massively elevated infiltration of $CD4^+$ and $CD8^+$ T cells in tumor tissues treated with anti-PD-1 or rhamnazin alone compared to vehicle group (Fig. 2A). Furthermore, the qRT-PCR results revealed that either anti-PD-1 or rhamnazin up-regulated CD4 and CD8 mRNA levels in tumor tissues, and the combination group
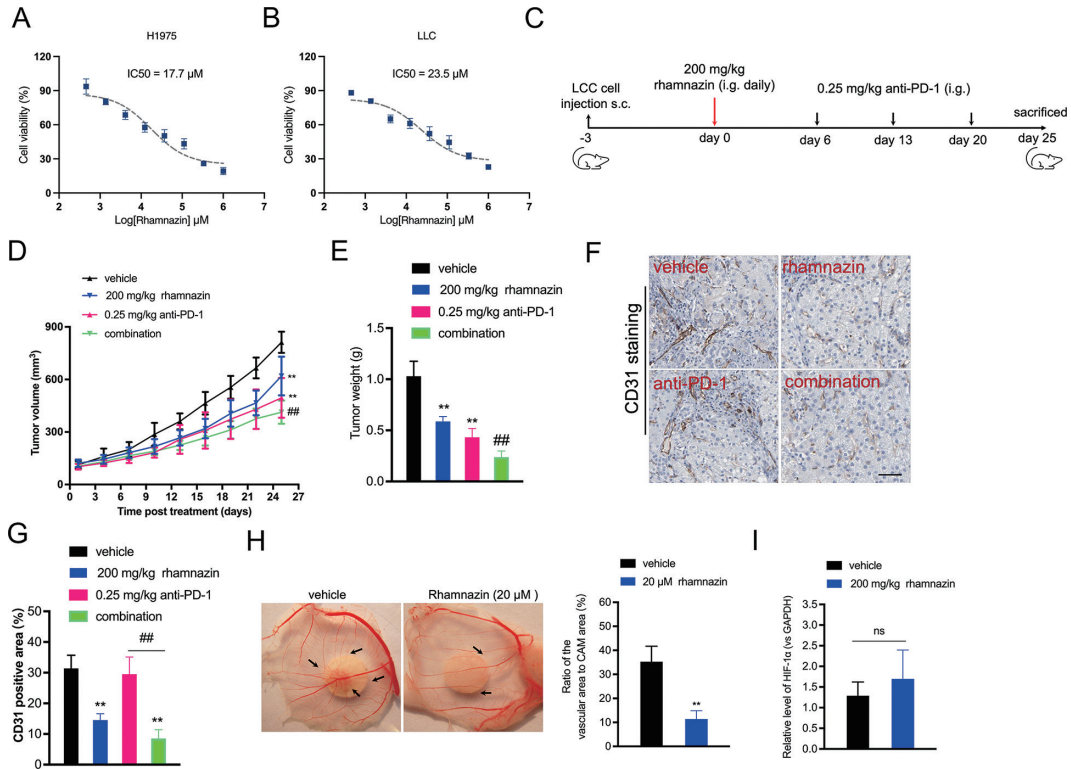
Fig. 1. Rhamnazin inhibits tumor growth and reduces angiogenesis in tumors with PD-1 blockade.
(A, B) Cell viability of H1975 and LLC cells was measured using the CCK-8 assay. (C) LLC xenografts were established in C57BL/6 mice by subcutaneous inoculation of LLC cells. Shematic diagram of modeling and treatment of rhamnazin and anti-PD-1 antibody in mice is shown. (D) The tumor volumes were measured every 3 days. 'Combination' represents a combination of 200 mg/kg rhamnazin and 0.25 mg/kg anti-PD-1. (E) After being sacrificed at day 25, the tumor weight was detected. (F) Representative images of IHC analysis by staining with anti-CD31 in tumor tissues. Scar bar = 100 μm. (G) Quantitative data of tumor angiogenesis. $^{**}p < 0.01$ compared with vehicle, $^{##}p < 0.001$ compared with anti-PD-1 group. (H) Blood vessels formed in representative images of the CAM assay after rhamnazin treatment. $^{**}p < 0.01$ compared with vehicle. (I) The mRNA level of HIF-1α in tumor tissue was assessed using qRT-PCR assay. Ns, no significant.

further enhanced these expressions than single-treated groups, illustrating that rhamnazin promoted infiltration of CD4$^+$ T and CD8$^+$ T cells in tumors with PD-1 blockade (Fig. 2B). In addition, increased percentage of proliferating (Ki67$^+$) CD8$^+$ T cells and CD69$^+$ CD8$^+$ T cells was induced by anti-PD-1 or rhamnazin, compared to the vehicle group. The combination treatment resulted in stronger effect on these T cell activation markers than single groups (Fig. 2C). To examine the immune status in tumors, we detected several expression levels of potent proinflammatory cytokines and mediators, including IFN-γ, TNF-α and granzyme B by ELISA. Treatment of anti-PD-1 or rhamnazin induced a significant increase of IFN-γ, TNF-α and granzyme B protein levels in tumors in comparison with vehicle group, and these levels were importantly higher in the combination group (Fig. 2D). These data suggested that anti-PD-1 therapy promoted T cell recruitment, activation, and activated local immune status, and the combined rhamnazin and anti-PD-1 further encouraged these anti-tumor immune activities.

Rhamnazin decreased PD-L1 expression in tumors of xenograft models

We next explored the effect of rhamnazin on PD-L1 expression in xenograft models or NSCLC cells. Based on the flow cytometry and western blot results, a significant decrease of PD-L1 level was observed in xenograft models with rhamnazin treatment or combination group, while there was no significant difference in PD-L1 level between anti-PD-1 and vehicle group (Fig. 3A, B). In H1975 cells, anti-PD-1 therapy had no noticeable impact on PD-L1 protein level, while the rhamnazin or combination treatment resulted in down-regulation of PD-L1 level (Fig. 3C, D). The above data indicated that administration of rhamnazin inhibited PD-L1 expression in mouse tumor tissues and NSCLC cells under PD-1 blockade condition.

Rhamnazin promotes T cell proliferation and enhanced production of cytotoxic mediators in the co-culture system

To determine the role of rhamnazin on T cell proliferation and production of cytotoxic mediators, naïve donor T cells in human PBMC were incubated with anti-CD3 antibody for the activation and then treated with rhamnazin. As
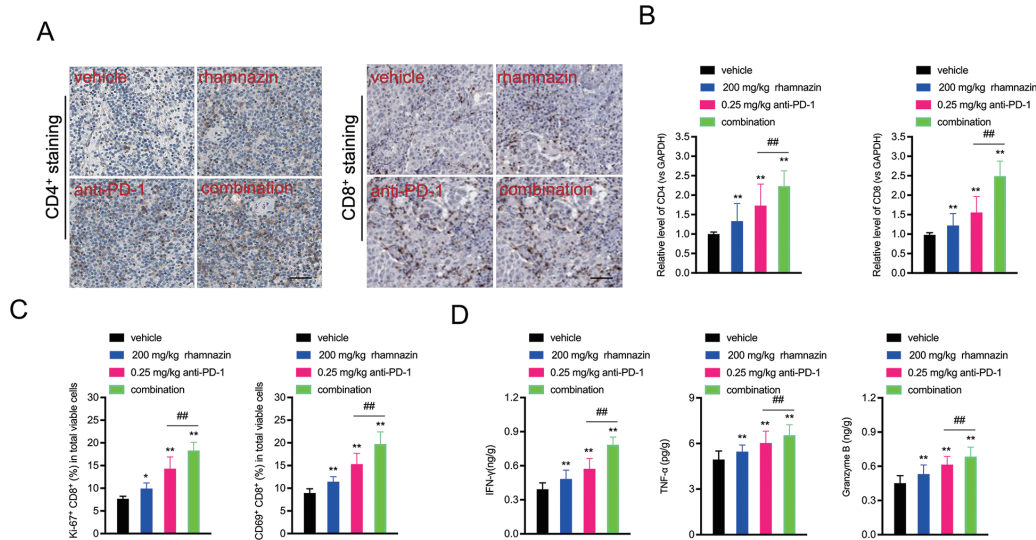
Fig. 2. Rhamnazin enhances T cell infiltration and activation, and activates local immune status in tumors with PD-1 block-ade.

The mouse Lewis xenografts were treated with rhamnazin or anti-PD-1 in the following. The animals were grouped as follows (n = 6): vehicle, rhamnazin, anti-PD-1, and a combination of rhamnazin and anti-PD-1 (combination). (A) Im-munohistochemical staining of $CD4^+$ and $CD8^+$ T cells in tumor tissues. Representative images in each group were shown. (B) Relative expressions of CD4 and CD8 in TILs were qualified by qRT-PCR. (C) The expression of activa-tion markers CD69 and Ki-67 on intra-tumor CD8 cells were assessed by flow cytometry. (D) The expressions of IFN-γ, TNF-α and granzyme B in tumors of mice were evaluated by ELISA. Scar bar = 100 μm. Similar cell results were obtained in three independent experiments. $^*p < 0.05$, $^{**}p < 0.01$ compared with vehicle; $^{##}p < 0.001$ compared with anti-PD-1 group.
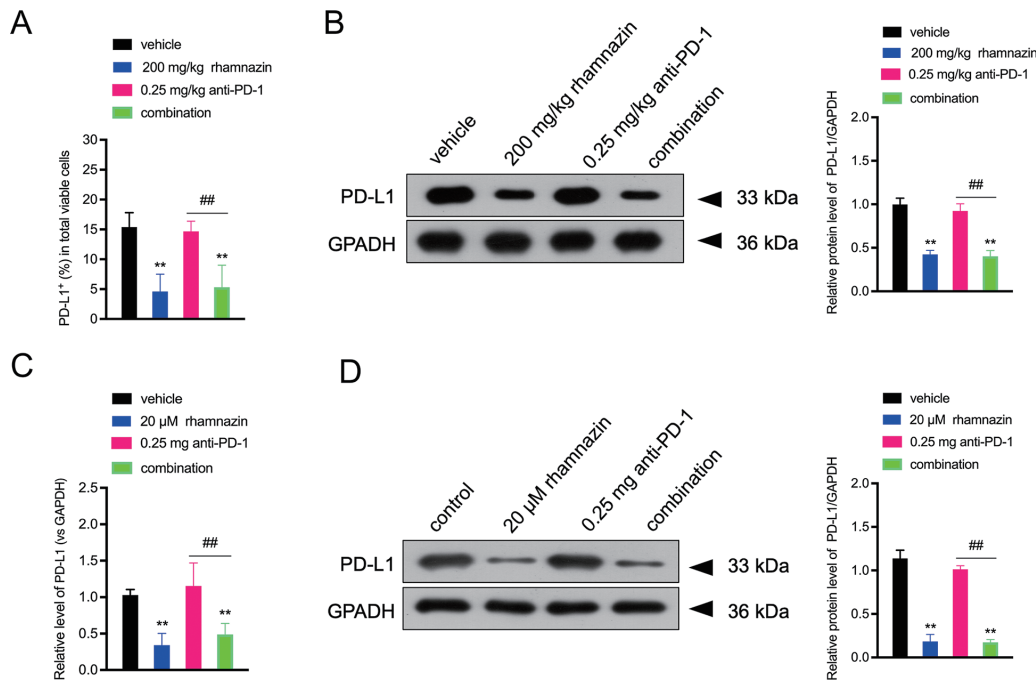

Fig. 3. Rhamnazin decreased PD-L1 expression in tumors of xenograft models and NSCLC cells.

The animals were grouped as follows (n = 6): vehicle, rhamnazin, anti-PD-1 and a combination of rhamnazin and anti-PD-1 (combination). (A) Percentage of PD-L1 positive staining in tumors of xenograft models was measured by flow cytometry. (B) PD-L1 protein level was measured in tumors of xenograft models by western blot. $^{**}p < 0.01$ compared with vehicle; $^{##}p < 0.001$ compared with anti-PD-1 group. (C, D) H1975 cells were incubated with rhamnazin (20 μM) with or without anti-PD-1 (0.25 mg) treatment for 24 h. Cells were allocated into 4 groups: Control, rhamnazin, anti-PD-1 and and a combination of rhamnazin and anti-PD-1 (combination). PD-L1 expression in H1975 cells was mea-sured by qRT-PCR and western blot. Similar cell results were obtained in three independent experiments. $^{**}p < 0.01$ compared with control; $^{##}p < 0.001$ compared with anti-PD-1 group.
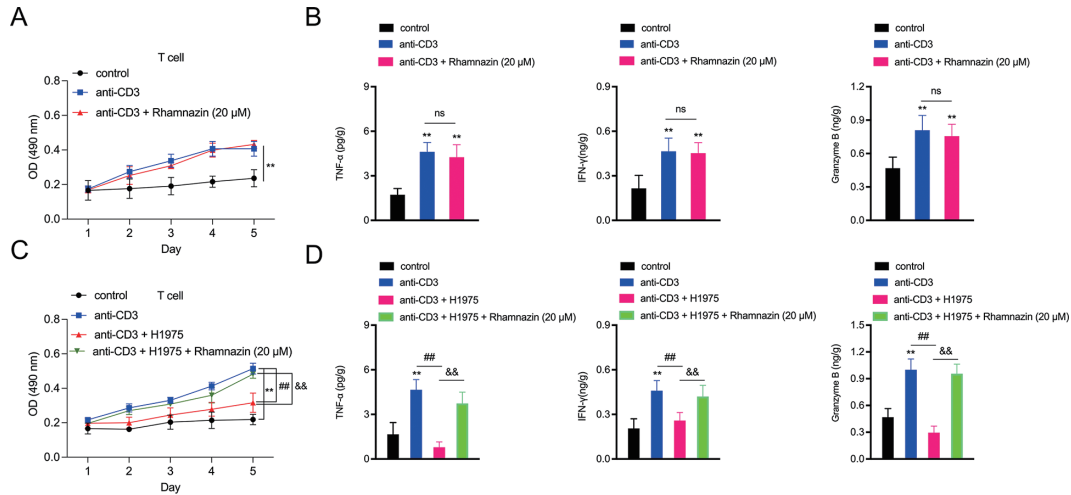
Fig. 4. Rhamnazin promotes T cell proliferation and cytotoxic factors production in the co-culture system.
The isolated T cells were incubated with anti-CD3 antibody followed by rhamnazin (20 μM) treatment for 24 h. Cells were assigned into 3 groups: Control, anti-CD3 and anti-CD3 + rhamnazin. CCK-8 assay (A), and ELISA (B) were carried out to determine the cell viability and concentrations of IFN-γ, TNF-α and granzyme B in the supernatants. $^{**}p <$ 0.01 compared with control. ns, no significant. (C, D) After being treated with anti-CD3 antibody or rhamnazin (20 μM), T cells were co-cultured with H1975 cells in a co-culture system for 24 h. T cell viability and concentrations of IFN-γ, TNF-α and granzyme B in supernatants were assessed by CCK-8 assay and ELISA. Similar cell results were obtained in three independent experiments. $^{**}p < 0.01$ compared with control; $^{##}p < 0.001$ compared with anti-CD3 group; $^{\&\&}p < 0.01$ compared with anti-CD3 + H1975 group.

shown in Fig. 4A, activated T cell proliferation was increased in a time-dependent manner, while rhamnazin had no significant direct effect on the T cell proliferation. Likewise, the concentrations of IFN-γ, TNF-α and granzyme B in supernatants were increased after T cell activation, while these levels showed no remarkable difference after rhamnazin treatment (Fig. 4B). Next, the activated T cells incubated with rhamnazin were co-cultured with H1975 cells to explore the indirect role of rhamnazin on T cell proliferation and cytotoxic factors production. After co-culturing, we confirmed the promotive role of rhamnazin on T cell proliferation, which manifested with a significant increase of OD value in comparison with anti-CD3 + H1975 group (Fig. 4C). Meanwhile, we discovered that rhamnazin markedly up-regulated cytotoxic mediators IFN-γ, TNF-α and granzyme B in T cell supernatants compared with the anti-CD3 + H1975 group (Fig. 4D).

Rhamnazin down-regulates PD-L1 expression in NSCLC cells through inhibiting phosphorylation of VEGFR2

To further explore whether rhamnazin regulates PD-L1 expression via regulation of VEGFR2 phosphorylation, H1975 cells were transfected with sh-VEGFR2 or VEGFR2-overexpression (VEGFR2-OE) and treated with VEGFA to activate VEGFR2 signaling. The western blot data confirmed the effective transfection of sh-VEGFR2 or VEGFR2-OE, and positive regulation of VEGFR2 on PD-L1 protein level (Fig. 5A, B). Next, VEGFR2-OE transfected H1975 cells were treated with rhamnazin and VEGFA. As shown in Fig. 5C, rhamnazin inhibited VEGFA-stimulated VEGFR2 phosphorylation and PD-L1

level whereas VEGFR2-OE transfection reversed these trends. In addition, rhamnazin had no obvious inhibitory effect on VEGFR2 phosphorylation and PD-L1 level in the presence of sh-VEGFR2 transfection (Fig. 5D). Finally, T cells stimulated with anti-CD3 and/or rhamnazin treatment were co-cultured with H1975 cells containing VEGFR2-OE transfection and VEGFA stimulation. Rhamnazin enhanced T cell proliferation and up-regulated cytotoxic mediators IFN-γ, TNF-α and granzyme B in T cell supernatants, whereas the VEGFR2-OE transfection in H1975 cells abrogated these changes (Fig. 5E, F). Taken together, these results suggest that rhamnazin down-regulates PD-L1 expression in NSCLC cells via inhibiting VEGFR2 phosphorylation, which in turn promotes T cell proliferation and enhanced cytotoxic mediator production.

Discussion

In recent years, the immunotherapy, especially the anti-PD-1 immunotherapy, has become a hot spot in cancer treatment, which is effective against various tumors and improves the 5-year survival rate of cancer patients (Reck et al. 2021; Nelson et al. 2022). Unfortunately, PD-1 antibodies have an obvious defect, that is, low efficiency. Nearly, an emerging treatment, the immunotherapy combined with anti-angiogenesis has attracted much attention, which clearly enhanced the anti-tumor effects of anti-PD-1 therapy in several human cancers (Hua et al. 2022; Pan et al. 2023). In this study, using a Lewis lung carcinoma model in C57BL/6 mice, we explored the effect of combined treatment of anti-angiogenic factor rhamnazin and anti-PD-1 therapy and the underlying mechanism. It was
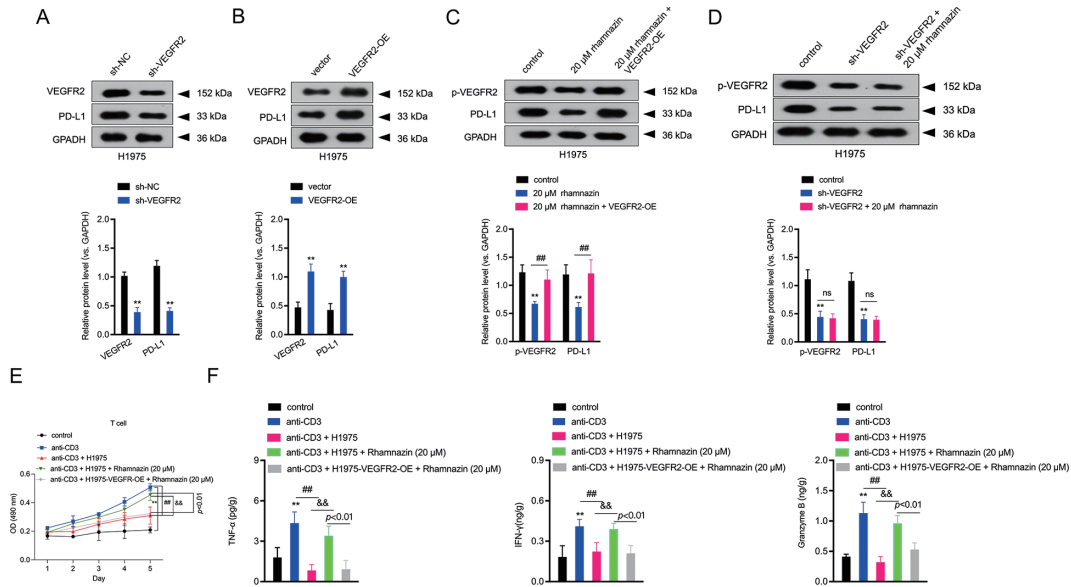
Fig. 5. Rhamnazin down-regulates PD-L1 expression in NSCLC cells through inhibiting phosphorylation of VEGFR2.
H1975 cells were transfected with sh-VEGFR2 or VEGFR2-OE, following by detection of VEGFR2 (A) and PD-L1(B) protein levels. sh-NC and empty vector were used as negative control. (C) H1975 cells were treated with rhamnazin (20 μM) and VEGFA (30 ng/ml) for 24 h, with or without prior VEGFR2-OE transfection. Protein levels of p-VEGFR2 and PD-L1 were measured. (D) H1975 cells were treated with rhamnazin (20 μM) and VEGFA (30 ng/ml) for 24 h, with or without prior sh-VEGFR2 transfection. Protein levels of p-VEGFR2 and PD-L1 were measured. (E, F) T cells stimulated with anti-CD3 and/or rhamnazin treatment were co-cultured with H1975 cells containing VEGFR2-OE transfection. Cells were allocated into 5 groups: control, anti-CD3, anti-CD3 + H1975, anti-CD3 + H1975 + rhamnazin and anti-CD3 + H1975-VEGFR2-OE + rhamnazin. T cell viability and concentrations of IFN-γ, TNF-α and granzyme B in supernatants were assessed by CCK-8 assay and ELISA. Similar cell results were obtained in three independent experiments. [**]$p < 0.01$ compared with control; [##]$p < 0.001$ compared with anti-CD3 group; [&&]$p < 0.01$ compared with anti-CD3 + H1975 group.

observed that, compared with the individual treated group, the combination of rhamnazin and anti-PD-1 markedly inhibited tumor growth, reduced angiogenesis in tumors, enhanced T cell infiltration and activation, and activated local immune status in tumors. *In vivo*, rhamnazin markedly reduced PD-L1 expression in tumors of xenograft models and H1975 cells. By co-culturing, rhamnazin promoted T cell proliferation and enhanced cytotoxic mediators production. Rhamnazin inhibited phosphorylation of VEGFR2 in H1975 cells, and the overexpression of VEGFR2 abolished the effect of rhamnazin on T cell proliferation and enhanced cytotoxic mediator production.

Emerging studies have confirmed the significant therapeutic approaches of combined immunotherapies and conventional treatments in cancers, in particular the anti-angiogenesis combined with anti-PD-1 therapy. For instance, the study by Cai et al. (2020) showed that the combined treatment of angiogenesis inhibitor apatinib and anti-PD-1 induced enhancement of anti-PD-1 anti-tumor efficacy in a mouse colon cancer model. Low-dose apatinib optimizes tumor microenvironment and potentiates anti-tumor effect of PD-1/PD-L1 blockade in lung cancer (Zhao et al. 2019). Yasuda et al. (2013) demonstrated that the simultaneous blockade of PD-1 and anti-angiogeneic regulator VEGFR2 induces synergistic anti-tumor effect in murine models. Rhamnazin has been confirmed having anti-angiogenic

activity and anti-tumor efficacy in human breast cancer (Yu et al. 2015). Based on this provided evidence, we explored whether rhamnazin could enhance the therapeutic efficacy of anti-PD-1 treatment. As expected, combination use of rhamnazin and anti-PD-1 inhibited the tumor growth more significant than anti-PD-1 or rhamnazin treatment alone, and rhamnazin alone or combined treatment dramatically induced anti-angiogenic effect compared to vehicle or anti-PD-1 group, suggesting that rhamnazin elevated the anti-tumor efficacy of anti-PD-1 therapy in LLC model mice. Likely, Zhao et al. (2019) demonstrated that the combined use of anti-angiogenic agent apatinib and PD-1/PD-L1 blockade changed the tumor microenvironment and potentiated anti-tumor effect in lung cancer compared to PD-1/PD-L1 blockade alone, which is consistent to our work on lung cancer.

It remains currently unknown whether combination of rhamnazin and anti-PD-1 treatment could also influence the tumor microenvironment (TEM) and immune status in lung cancer. In this study, we observed that combined treatment of anti-PD-1 and rhamnazin showed a more prominent increase of CD4^{+} T and CD8^{+} T cell infiltration, increased CD4 and CD8 expressions, and elevation of the percentage of proliferating (Ki67^{+}) CD8^{+} T cells and CD69^{+} CD8^{+} T cells compared to the anti-PD-1 and rhamnazin treated alone. TNF-α is a significant inflammatory cytokine pro-
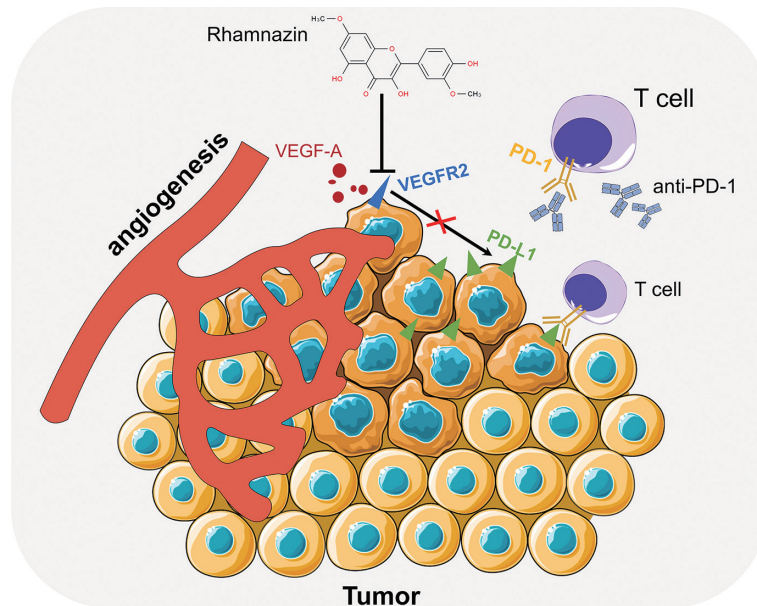
Fig. 6. Schematic of rhamnazin affecting efficacy of anti-PD-1 therapy for lung cancer.
Rhamnazin inhibits VEGFA-stimulated phosphorylation of VEGFR2 and then reduces PD-L1 expression in NSCLC cells, which in turn promotes the T cell proliferation and cytotoxic factors production.

duced by activated immune cells, including T cells during acute inflammation (Idriss and Naismith 2000). IFN-γ is mainly produced by activated T cells (Kimura et al. 2010). Granzyme B is mainly released from cytotoxic T lymphocytes and can provoke tumor cell death via various pathways (Ritter et al. 2022). We detected these inflammatory mediators in tumor tissues to assess the local immune status. The result showed that the combined treatment induced higher IFN-γ, TNF-α and granzyme B protein levels in tumor tissues than single treated groups. These data suggest that the combined rhamnazin and anti-PD-1 have a stronger effect on promoting T cell recruitment, activation, and activation of local immune status than anti-PD-1 therapy alone. The combining PD-1 blockade and rhamnazin may exert anti-tumor efficacy through controlling TEM by promoting T cell infiltration and inducing activation of local immune response.

Studies have shown that the PD-L1/PD-1 pathway has a significant role in tumor immunity, and its blockade has a therapeutic potential against many cancers (Chen et al. 2020b). PD-1 mediated an inhibitory effect when binding to its ligand PD-L1 or PD-L2 (Concha-Benavente et al. 2018). This study found that PD-L1 expression was significantly decreased in tumor tissues of LLC model and NSCLS cell line when treated with rhamnazin. The VEGFA/VEGFR2 signal is an interesting area for combined angiogenic therapy approaches, and this signal mediates the suppressive effect of anti-tumor immune response (Patten et al. 2010). As previously described, rhamnazin is an inhibitor of VEGFR2 signaling with potent anti-angiogenic activity and anti-tumor efficacy (Yu et al. 2015). Several preclinical studies have observed promising anti-tumor effects from anti-angiogenic agents combined with immunothera-

pies in multiple tumor types such as melanoma, renal cell carcinoma, and colon adenocarcinoma (Zhao et al. 2019). In our work, we confirmed that rhamnazin reduced VEGFA-stimulated phosphorylation of VEGFR2, promoted T cell proliferation and enhanced production of cytotoxic mediators IFN-γ, TNF-α and granzyme B in the co-culture system, while constitutive VEGFR2 overexpression significantly reversed the effect of rhamnazin on PD-L1 expression, T cell proliferation and production of cytotoxic mediators. The above data suggest that rhamnazin induces down-regulation of PD-L1 expression, T cell proliferation and cytotoxic effects through inhibition of VEGFR2 phosphorylation in lung cancer cells. Further studies need to be carried out to determine the phosphorylation site of rhamnazin on VEGFR2 and the molecular mechanisms of VEGFA-VEGFR2 axis in PD-L1 expression regulation. Recently, it has been shown that T cell-induced tumor cell ferroptosis, a non-apoptotic, iron-dependent form of programmed cell death, contributes to T cell-mediated tumor eradication during immunotherapy (Jiang et al. 2021). Dysregulated ferroptosis-related genes indicate the potential clinical benefits for anti-PD-1/PD-L1 immunotherapy in lung adenocarcinoma (Zhou et al. 2021). Mechanistically, immunotherapy-activated CD8^{+} T cells enhance ferroptosis-specific lipid peroxidation in tumor cells, and that increased ferroptosis contributes to the anti-tumor efficacy of immunotherapy (Wang et al. 2019). Rhamnazin inhibits hepatocellular carcinoma cell aggressiveness *in vitro* via inducing ferroptosis (Mei et al. 2022). It remains to be elucidated whether rhamnazin improves the immunosuppressive tumor microenvironment via inducing ferroptosis.

Overall, this study demonstrated that rhamnazin enhanced the anti-tumor efficacy of anti-PD-1 therapy in

Lewis lung carcinoma xenograft. Its anti-tumor effects may be affected by alternation of T cell infiltration and local immune activation via regulating of PD-L1 expression and phosphorylation of VEGFR2 (Fig. 6). Therefore, the combination of rhamnazin and anti-PD-1 may be a potential therapy for lung cancer.

Conflict of Interest

The authors declare no conflict of interest.

References

Belgore, F., Blann, A., Neil, D., Ahmed, A.S. & Lip, G.Y. (2004) Localisation of members of the vascular endothelial growth factor (VEGF) family and their receptors in human atherosclerotic arteries. *J. Clin. Pathol.*, **57**, 266-272.

Cai, X., Wei, B., Li, L., Chen, X., Liu, W., Cui, J., Lin, Y., Sun, Y., Xu, Q., Guo, W. & Gu, Y. (2020) Apatinib enhanced anti-PD-1 therapy for colon cancer in mice via promoting PD-L1 expression. *Int. Immunopharmacol.*, **88**, 106858.

Chang, C.C., Chuang, C.L., Lee, F.Y., Wang, S.S., Lin, H.C., Huang, H.C., Teng, T.H., Hsu, S.J., Hsieh, H.G. & Lee, S.D. (2013) Sorafenib treatment improves hepatopulmonary syndrome in rats with biliary cirrhosis. *Clin. Sci. (Lond.)*, **124**, 457-466.

Chen, D.S. & Mellman, I. (2017) Elements of cancer immunity and the cancer-immune set point. *Nature*, **541**, 321-330.

Chen, L. & Han, X. (2015) Anti-PD-1/PD-L1 therapy of human cancer: past, present, and future. *J. Clin. Invest.*, **125**, 3384-3391.

Chen, Q., Yu, W.Y., Zhang, H.H., Zhang, S.Z., Fang, J., Wu, F., Ying, H.Z. & Yu, C.H. (2020a) PBX3 promotes tumor growth and angiogenesis via activation of AT1R/VEGFR2 pathway in papillary thyroid carcinoma. *Biomed Res. Int.*, **2020**, 8954513.

Chen, X., Pan, X., Zhang, W., Guo, H., Cheng, S., He, Q., Yang, B. & Ding, L. (2020b) Epigenetic strategies synergize with PD-L1/PD-1 targeted cancer immunotherapies to enhance antitumor responses. *Acta Pharm. Sin. B*, **10**, 723-733.

Concha-Benavente, F., Kansy, B., Moskovitz, J., Moy, J., Chandran, U. & Ferris, R.L. (2018) PD-L1 mediates dysfunction in activated PD-1(+) NK cells in head and neck cancer patients. *Cancer Immunol. Res.*, **6**, 1548-1560.

Elice, F. & Rodeghiero, F. (2012) Side effects of anti-angiogenic drugs. *Thromb. Res.*, **129** Suppl 1, S50-53.

Hegde, P.S., Karanikas, V. & Evers, S. (2016) The where, the when, and the how of immune monitoring for cancer immunotherapies in the era of checkpoint inhibition. *Clin. Cancer Res.*, **22**, 1865-1874.

Hu, J., Wang, W., Liu, C., Li, M., Nice, E. & Xu, H. (2019) Receptor tyrosine kinase inhibitor Sunitinib and integrin antagonist peptide HM-3 show similar lipid raft dependent biphasic regulation of tumor angiogenesis and metastasis. *J. Exp. Clin. Cancer Res.*, **38**, 381.

Hua, Y., Dong, R., Jin, T., Jin, Q. & Chen, X. (2022) Anti-PD-1 monoclonal antibody combined with anti-VEGF agent is safe and effective in patients with recurrent/metastatic head and neck squamous cancer as second-line or beyond treatment. *Front. Oncol.*, **12**, 781348.

Idriss, H.T. & Naismith, J.H. (2000) TNF alpha and the TNF receptor superfamily: structure-function relationship(s). *Microsc. Res. Tech.*, **50**, 184-195.

Jiang, Z., Lim, S.O., Yan, M., Hsu, J.L., Yao, J., Wei, Y., Chang, S.S., Yamaguchi, H., Lee, H.H., Ke, B., Hsu, J.M., Chan, L.C., Hortobagyi, G.N., Yang, L., Lin, C., et al. (2021) TYRO3 induces anti-PD-1/PD-L1 therapy resistance by limiting innate immunity and tumoral ferroptosis. *J. Clin. Invest.*, **131**, e139434.

Kimura, D., Miyakoda, M., Honma, K., Shibata, Y., Yuda, M., Chinzei, Y. & Yui, K. (2010) Production of IFN-γ by CD4(+) T cells in response to malaria antigens is IL-2 dependent. *Int. Immunol.*, **22**, 941-952.

Losanno, T., Rossi, A., Maione, P., Napolitano, A. & Gridelli, C. (2016) Anti-EGFR and antiangiogenic monoclonal antibodies in metastatic non-small-cell lung cancer. *Expert Opin. Biol. Ther.*, **16**, 747-758.

Mahoney, K.M., Rennert, P.D. & Freeman, G.J. (2015) Combination cancer immunotherapy and new immunomodulatory targets. *Nature reviews. Drug discovery*, **14**, 561-584.

Martini, N.D., Katerere, D.R. & Eloff, J.N. (2004) Biological activity of five antibacterial flavonoids from Combretum erythrophyllum (Combretaceae). *J. Ethnopharmacol.*, **93**, 207-212.

Mei, F., Liu, Y. & Zheng, S. (2022) Rhamnazin inhibits hepatocellular carcinoma cell aggressiveness in vitro via glutathione peroxidase 4-dependent ferroptosis. *Tohoku J. Exp. Med.*, **258**, 111-120.

Nelson, A., Gebremeskel, S., Lichty, B.D. & Johnston, B. (2022) Natural killer T cell immunotherapy combined with IL-15-expressing oncolytic virotherapy and PD-1 blockade mediates pancreatic tumor regression. *J. Immunother. Cancer*, **10**, e003923.

Pan, M., Wang, F., Nan, L., Yang, S., Qi, J., Xie, J., Shao, S., Zou, H., Wang, M., Sun, F. & Zhang, J. (2023) αVEGFR2-MICA fusion antibodies enhance immunotherapy effect and synergize with PD-1 blockade. *Cancer Immunol. Immunother.*, **72**, 969-984.

Patten, S.G., Adamcic, U., Lacombe, K., Minhas, K., Skowronski, K. & Coomber, B.L. (2010) VEGFR2 heterogeneity and response to anti-angiogenic low dose metronomic cyclophosphamide treatment. *BMC Cancer*, **10**, 683.

Reck, M., Rodriguez-Abreu, D., Robinson, A.G., Hui, R., Csoszi, T., Fulop, A., Gottfried, M., Peled, N., Tafreshi, A., Cuffe, S., O'Brien, M., Rao, S., Hotta, K., Leal, T.A., Riess, J.W., et al. (2021) Five-year outcomes with pembrolizumab versus chemotherapy for metastatic non-small-cell lung cancer with PD-L1 tumor proportion score >/= 50. *J. Clin. Oncol.*, **39**, 2339-2349.

Relli, V., Trerotola, M., Guerra, E. & Alberti, S. (2019) Abandoning the notion of non-small cell lung cancer. *Trends Mol. Med.*, **25**, 585-594.

Ritter, A.T., Shtengel, G., Xu, C.S., Weigel, A., Hoffman, D.P., Freeman, M., Iyer, N., Alivodej, N., Ackerman, D., Voskoboinik, I., Trapani, J., Hess, H.F. & Mellman, I. (2022) ESCRT-mediated membrane repair protects tumor-derived cells against T cell attack. *Science*, **376**, 377-382.

Vansteenkiste, J., Wauters, E., Reymen, B., Ackermann, C.J., Peters, S. & De Ruysscher, D. (2019) Current status of immune checkpoint inhibition in early-stage NSCLC. *Ann. Oncol.*, **30**, 1244-1253.

Volz, C., Breid, S., Selenz, C., Zaplatina, A., Golfmann, K., Meder, L., Dietlein, F., Borchmann, S., Chatterjee, S., Siobal, M., Schottle, J., Florin, A., Koker, M., Nill, M., Ozretic, L., et al. (2020) Inhibition of tumor VEGFR2 induces Serine 897 EphA2-dependent tumor cell invasion and metastasis in NSCLC. *Cell Rep.*, **31**, 107568.

Wang, W., Green, M., Choi, J.E., Gijon, M., Kennedy, P.D., Johnson, J.K., Liao, P., Lang, X., Kryczek, I., Sell, A., Xia, H., Zhou, J., Li, G., Li, J., Li, W., et al. (2019) CD8(+) T cells regulate tumour ferroptosis during cancer immunotherapy. *Nature*, **569**, 270-274.

Xia, L., Liu, Y. & Wang, Y. (2019) PD-1/PD-L1 blockade therapy in advanced non-small-cell lung cancer: current status and future directions. *Oncologist*, **24**, S31-S41.

Yasuda, S., Sho, M., Yamato, I., Yoshiji, H., Wakatsuki, K., Nishiwada, S., Yagita, H. & Nakajima, Y. (2013) Simultaneous blockade of programmed death 1 and vascular endothelial

growth factor receptor 2 (VEGFR2) induces synergistic anti-tumour effect in vivo. *Clin. Exp. Immunol.*, **172**, 500-506.

Yu, H. & Li, S.B. (2020) Role of LINC00152 in non-small cell lung cancer. *J. Zhejiang Univ. Sci. B*, **21**, 179-191.

Yu, Y., Cai, W., Pei, C.G. & Shao, Y. (2015) Rhamnazin, a novel inhibitor of VEGFR2 signaling with potent antiangiogenic activity and antitumor efficacy. *Biochem. Biophys. Res. Commun.*, **458**, 913-919.

Yu, Y., Zhou, X.Z., Ye, L., Yuan, Q., Freeberg, S., Shi, C., Zhu, P.W., Bao, J., Jiang, N. & Shao, Y. (2018) Rhamnazin attenuates inflammation and inhibits alkali burn-induced corneal neovascularization in rats. *RSC Adv.*, **8**, 26696-26706.

Zhao, S., Ren, S., Jiang, T., Zhu, B., Li, X., Zhao, C., Jia, Y., Shi, J., Zhang, L., Liu, X., Qiao, M., Chen, X., Su, C., Yu, H., Zhou, C., et al. (2019) Low-dose apatinib optimizes tumor microenvironment and potentiates antitumor effect of PD-1/PD-L1 blockade in lung cancer. *Cancer Immunol. Res.*, **7**, 630-643.

Zhou, M., Zhang, X., Li, T. & Chen, Y. (2021) Dysregulated ferroptosis-related genes indicate potential clinical benefits for anti-PD-1/PD-L1 immunotherapy in lung adenocarcinoma. *J. Clin. Lab. Anal.*, **35**, e24086.

———————————